Experimental and Computational Multiphase Flow
Vol. 4, No. 4, 2022, 389–398
https://doi.org/10.1007/s42757-022-0142-x

Analysis of occupants' exposure risk of cough-expelled droplets in the workspace with various mixing ventilation layouts

Xiang Fang[1,2], Xueren Li[2], Yihuan Yan[1] (✉), Yao Tao[1,2], Ziqi Chen[2], Ping Yan[1] (✉)

1. School of Air Transportation/Flying, Shanghai University of Engineering Science, Shanghai 201620, China
2. School of Engineering, RMIT University, PO Box 71, Bundoora, VIC 3083, Australia

Abstract

This study numerically investigated the transport characteristics of the cough-expelled droplets and their corresponding exposure risk of each occupant under various mixing ventilation layouts. Transient simulations were conducted in a conference room, while pathogen-bearing droplets were released by a standing speaker. The results showed that droplet residues (< 40 μm) had a high potential to reach occupant's breathing zone, among which the number fraction of aerosol residues (< 10 μm) could be nearly doubled compared with that of the rest droplet residues in the breathing zone. Occupants' exposure risks were found very sensitive to the ventilation layouts. The strong ventilated flow could significantly promote droplet dispersions when those inlets were closely located to the infectious speaker, resulting in all occupants exposed to a considerable fraction of aerosols and droplets within a given exposure time of 300 s. The mixing ventilation layout did not have a consistent performance on restricting the pathogen spread and controlling the occupant's exposure risk in an enclosed workspace. Its performance could be highly sensitive to the location of the infectious agent. Centralized vent layouts could provide relatively more consistent performance on removing droplets, whilst some local airflow recirculation with locked droplets were noticed.

Keywords

cough-expelled droplets
conference room
occupant's safety and health
droplet exposure risk

Article History

Received: 11 July 2022
Accepted: 21 July 2022

Research Article

1 Introduction

The outbreak of transmissible respiratory disease, COVID-19, has wreaked havoc on human society and hindered the rapid growth of the economy in the recent two years. Compared to the previous respiratory disease (e.g., SARs), this respiratory pathogen is highly contagious and capable of mutating into new variants (i.e., Delta and Omicron) (Wang et al., 2021). Because of the biological characteristics of these pathogens, pharmaceutical interventions such as vaccines were unable to fully contain the pandemics (Katella, 2021). As a consequence, global pandemic waves caused more than half a billion confirmed cases and 6 million deaths until June 1, 2022 (Johns Hopkins University, 2020). With the rising severity of the airborne respiratory disease being identified from the ongoing outbreaks, more emphasis has been placed on these non-pharmaceutical interventions, such as indoor ventilation, HVAC setup, masks, social distance rule, etc. (Anderson et al., 2020; Sohrabi et al., 2020). These interventions are regulated largely based on the key mechanism of the droplet and fluid dynamics, which can be carefully mediated from the overall transmission process (i.e., exhalation, suspension, inhalation, and deposition) (Mittal et al., 2020). During this uncertain but vital period, any intervention strategy could be valuable in slowing the rapid spread of the deadly virus. Thus, understanding the droplets and fluid dynamics would better serve such purpose and the knowledge would be crucial for risk assessment and disease prevention related to droplet exposure.

Infectious pathogens are carried in human mucus and are transmitted through three major routes: fomite, close contact, and airborne in the form of droplets through human respiratory behavior (e.g., speaking, coughing, and sneezing) (World Health Organization, 2021). These transmission routes are strongly related to the intensity of respiratory flows and the number of pathogen-bearing

✉ Y. Yan, yihuan.yan@outlook.com; P. Yan, ping.yan@sues.edu.cn

droplets ejected. The first two transmission routes can be effectively prevented by implementing the social distance rule and frequent sanitization, whereas these measures have a very limited effect on containing airborne transmission because small droplets ejected into the local environment can linger in the air for an extended period of time and distance (World Health Organization, 2020b). During the droplet releasing period, strong respiratory behavior (e.g., coughing and sneezing) can generate a wild jet flow with a peak velocity of more than 10 m/s, which vastly dominates the droplet's initial process (Wei and Li, 2015). When these small droplets are released with the cough or sneeze flow, the strong jet effect would break the local airflow by generating intensive flow vortex around the jet. Due to the insignificant weight of these airborne droplets (< 5–10 μm), they could be easily trapped into the vortex regions with extended travelling time in the air compared to the rapidly settled large droplets (Greenhalgh et al., 2021). Therefore, to comprehensively assess the respiratory disease transmission, especially for airborne route, the key knowledge of the droplet and respiratory flow characteristic during the exhalation process should be carefully understood.

Due to the aforementioned characteristic of aerosols, airborne transmission poses a greater risk to the public than the other two transmission routes. As the fate of these small aerosol droplets is largely dominated by the local flow field, more attentions have been frequently put to the characteristics of the indoor ventilations (e.g., layout, rate, etc.) (Lipinski et al., 2020). Increasing ventilation rate is found as one of the possible solutions to limit the fast spread of the virus as the localised pathogens can be discharged with a higher ventilation rate (Anderson et al., 2020). However, this could lead to large concerns with respect to the high energy consumption as surplus air supply may be sometimes unnecessary within low pathogen concentration condition, and thus more focus has been put on the ventilation schemes (Allen and Ibrahim, 2021). Mixing ventilation, as the most widely used ventilation scheme in the indoor and built environment, has long been well-known for its benefits in improving the indoor air quality by distributing well-mixed airflow pattern in the indoor space (Fan et al., 2017). However, even though such ventilation scheme could effectively distribute the fresh air throughout the occupied space and ensure each occupant experience similar air quality, recent evidence demonstrated that mixing ventilation could potentially promote the spread of the infectious pathogen indoors (Lu et al., 2020; Miller et al., 2021). With the ongoing pandemic raising concerns about the effectiveness of indoor ventilation, more emphasis should be placed on designing an optimal ventilation system.

Repetitive emerging evidence revealed that occupants working in a densely occupied enclosed workspace could face a significantly higher biological and infection risk than others (World Health Organization, 2020a; Carvalhais et al., 2021). These workspace designs generally preclude effective social distance, mandatory mask regulation but absent or very limited ventilations. To effectively minimise the health risk for occupants, environmental health practice, including risk assessment, control, and prevention of a hazard, must first be thoroughly researched. Among these, risk assessment in relation to human exposure to infectious droplets play a vital role in the early stage of the disease transmission investigation (Nicas et al., 2005). Due to the human exposure risk is closely linked to the occupants exposed to pathogen-bearing droplets for a given time period that is influenced by various affecting factors (e.g., ventilation), it could be a good reference to reflect the effectiveness of the implemented measures (Motamedi et al., 2022). Recently, with the increasing demand for conducting a robust and fast evaluation of human indoor exposure risks, the use of CFD-based simulation is becoming more popular as it can cost-effectively assess the exposure risk by visualising detailed droplet trajectories (Peng et al., 2020).

Therefore, to broaden the understanding of the safety and health of the occupants in the indoor environment, this study numerically investigated widely employed mixing ventilation schemes by distributing the vents in a conference room with five different layouts. Natural ventilation conditions (i.e., with the door open) were also tested for comparison. Cough, one of the most common respiratory activities, was modelled based on the experimental measurement from the literature. Cough contaminants were ejected with jet flow from the standing speaker's mouth and the detailed droplet trajectories were tracked using the Eulerian–Lagrangian framework. Nine occupants were designated as susceptible individuals, and their exposure risks within ventilation conditions were carefully evaluated.

2 Method

2.1 CFD model and boundary conditions

A conference room with dimensions of 9 m (length) × 6.4 m (width) × 3 m (height) was numerically constructed for the purpose of investigation, as illustrated in Fig. 1. All the room walls were assumed to be adiabatic and air with a constant temperature of 20 °C was supplied from the vents located at the top ceiling of the room according to the ASHARE standard (ASHRAE, 2011). A total of 16 vents with 4 × 4 arrangement were used in this study and various combinations of the mixing ventilation layouts were thereupon developed, as summarized in Table 1.

Case 1 was the benchmark case in which the ventilation was not activated. The airflow naturally entered or exited

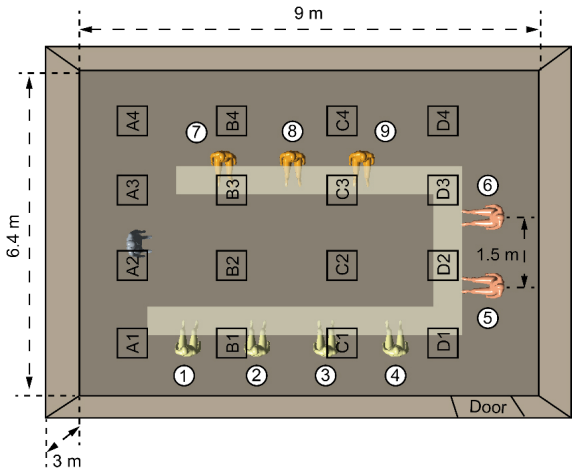

Fig. 1 Computational domain.

from the main door. The ventilations applied in Cases 2, 3, and 4 were traditional mixing ventilation schemes, which was widely applied in a typical conference room (Lipinski et al., 2020). In Cases 5 and 6, the mixing ventilations with centralized vent layouts were proposed. These two ventilations were based on the idea of centralising or decentralising the local airflow in the occupant's local environment, aiming to accelerate the movement of the contaminants in these lock-up regions. The air exchange rate was carefully regulated to be 8 h^{-1} (Sheriff, 2020), which yielded an air supply rate of 0.12 kg/s at the inlets.

To restore the real working scenario, a standing speaker with detailed body features was numerically built as the infectious agent and nine participants with seating postures were constructed as the susceptible listeners. The body features of each manikin were mostly retained as our previous study found that oversimplification of manikin model could yield uncertainty when predicting the exposure risks of individuals (Yan et al., 2016). As human thermal plume plays a vital role in affecting the droplet movement in the vicinity of the occupants, the heat release rate of the manikin body was carefully set as 45 W based on the experimental results conducted by Licina et al. (2014). Saliva droplets with a density of 1000 kg/m^3 containing 1.8% of pathogens were released from the stranding speaker's mouth. The cough flow rate and size distribution of the cough droplet were based on the experimental measurement conducted by Gupta et al. (2009) and Chao et al. (2009), respectively, as illustrated in Fig. 2.

The entire domain, including manikins, TV, and table were discretized using unstructured tetrahedron mesh, in which the meshing process was conducted in ICEM 2021 R1. Ten inflation layers with an initial height of 1 mm were employed at the proximity of the obstacles' surface to capture the detailed gradient of critical parameter, such as velocity and temperature. Natural ventilation case was used for mesh independence test. Four mesh configurations of 4, 6, 8, and 10 million, were employed respectively. The mesh independence was achieved at the 8 million elements with less than 5% of prediction deviation found with further increase of the mesh elements.

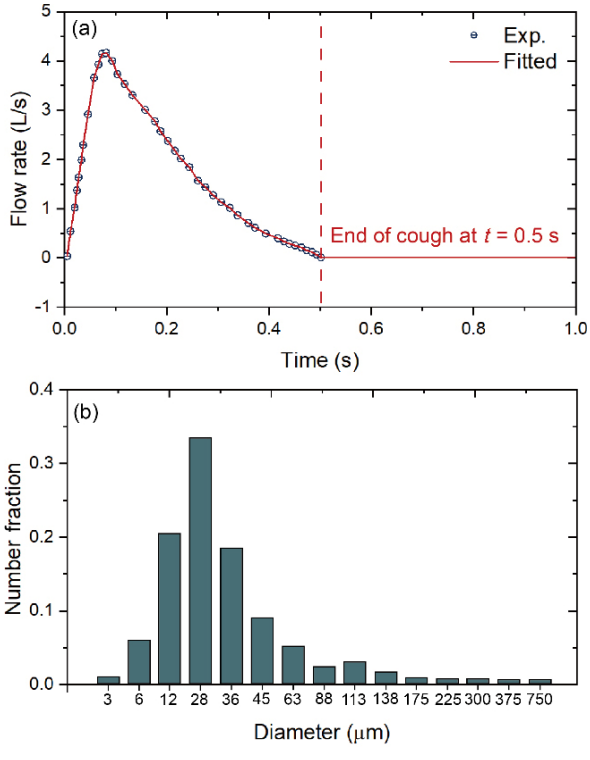

Fig. 2 (a) Cough flow rate and (b) number fraction of released cough droplets.

Table 1 Case description

	Case 1	Case 2	Case 3
Name	No ventilation (door open)	Mixed Ventilation 1 (MV1)	Mixed Ventilation 2 (MV2)
	In: No vents	**In**: A1, B1, C1, D1	**In**: A1, A2, A3, A4
	Out: Door	**Out**: A4, B4, C4, D4	**Out**: D1, D2, D3, D4
	Case 4	Case 5	Case 6
Name	Mixed Ventilation 3 (MV3)	Centralized Ventilation 1 (CV1)	Centralized Ventilation 2 (CV2)
	In: D1, D2, D3, D4	**In**: A1, A4, D1, D4	**In**: B2, B3, C2, C3
	Out: A1, A2, A3, A4	**Out**: B2, B3, C2, C3	**Out**: A1, A4, D1, D4

Six transient simulations considering the coughing scenarios were further calculated based on the steady-state results of each ventilation configuration. The movement of droplets was continuously tracked using the Eulerian–Lagrangian particle tracking framework. These expelled cough droplets would be fully deposited on the wall once they hit it. A small time-step of 0.01 s was applied at the initial cough releasing period, and a total time of 300 s droplet tracking was performed for each case, which took approximately 100 h to parallelly finish each case using a workstation with 40 CPU cores and 128 GB RAM.

2.2 Mathematic equations

In this study, the re-normalisation group (RNG) k–ε model was selected to capture airflow turbulence due its well-reputation in predicting the indoor airflow pattern and contaminant distributions (Chen, 1995). Based on the Reynolds-Averaged Navier–Stokes (RANS) framework, the movement and heat transfer of the fluid flow can be solved by the continuity, momentum, and energy equation (Eqs. (1)–(3)):

$$\frac{\partial}{\partial t}\rho + \nabla\cdot(\rho\vec{U}) = 0 \tag{1}$$

$$\frac{\partial}{\partial t}(\rho\vec{U}) + \nabla\cdot\left(\rho\vec{U}\vec{U} - \mu\left(\nabla\vec{U} + (\nabla\vec{U})^{\mathrm{T}}\right)\right) = S_{\mathrm{Buoy}} - \nabla p \tag{2}$$

$$\frac{\partial}{\partial t}(\rho H) + \nabla\cdot(\rho H\vec{U} - \nabla(\lambda T)) = \sum_{i=1}^{N}[\pi d^2 h(T_{\mathrm{m}} - T_{\mathrm{d}})] \tag{3}$$

where ρ is the density, p is the pressure, $\vec{U}$ is the mass-averaged velocity, H is the enthalpy, μ is the viscosity, λ is the thermal conductivity, and d is the droplet diameter. T_{d} and T are the droplet temperature and fluid temperature, respectively, and T_{m} is the mixture temperature. h is the interfacial heat transfer coefficient. The source term S_{Buoy} represents the momentum source due to buoyancy.

In the Eulerian–Lagrangian framework, the effect of turbulent dispersion on droplet transport is modelled by additionally considering the eddy fluctuating component of the air velocity onto the mean air velocity. This fluctuating component of the air velocity mainly governs the droplet movement in the turbulent flow region. The equation of local air velocity can be expressed as

$$\vec{U}_{\mathrm{a}} = \bar{U}_{\mathrm{a}} + \Phi\left(\frac{2k}{3}\right)^{0.5} \tag{4}$$

where Φ is a normally distributed random number which accounts for the randomness of turbulence about a mean value.

For a continuous flow carrying a discrete phase, significant forces on droplet motion are mainly drag and buoyancy force, F_{D} and F_{B}, respectively, which can be expressed as

$$m_{\mathrm{p}}\frac{\mathrm{d}\bar{U}_{\mathrm{p}}}{\mathrm{d}t} = \vec{F}_{\mathrm{D}} + \vec{F}_{\mathrm{B}} \tag{5}$$

$$\vec{F}_{\mathrm{D}} = \frac{C_{\mathrm{D}}}{2}\frac{\pi d_{\mathrm{p}}^2}{4}\rho_{\mathrm{a}}\left|\vec{U}_{\mathrm{p}} - \vec{U}_{\mathrm{a}}\right|\left(\vec{U}_{\mathrm{p}} - \vec{U}_{\mathrm{a}}\right) \tag{6}$$

$$\vec{F}_{\mathrm{B}} = \frac{\pi d_{\mathrm{p}}^3}{6}(\rho_{\mathrm{p}} - \rho_{\mathrm{a}})g \tag{7}$$

3 Results and discussion

3.1 Airflow field

Figure 3 depicts the airflow patterns produced by the six ventilation strategies. A velocity profile at 0.25 m above the speaker's head was first visualised to reveal the impact of the ventilated flow in the individual's local environment. As illustrated in Fig. 3, the velocity profile of the human thermal plume was uniform without the ventilation turned on, with a velocity ranging from 0.18 to 0.24 m/s (i.e., red - 0.24 m/s, green - 0.21 m/s, and blue - 0.18 m/s). The maximum velocity was observed at the center and quickly dissipated to the surrounding area, and the overall pattern was found to be highly consistent with the experimental measurements carried by Licina et al. (2014). With the inclusion of the ventilation, the strong ventilated jet flow could largely distort the thermal plume pattern, implying that the ventilation flow interacted very intensely with the individual's local environment.

The airflow pattern could be highly stagnant without the inclusion of ventilation. It can be clearly found that in Case 1, the airflow was mainly governed by the thermally driven buoyancy flow. In comparison, the movement of airflow could become more intense with traditional mixing ventilation (i.e., MV 1, MV 2, and MV 3) and more frequent interaction between the turbulent jet flow and obstacles was clearly observed among the cases. These localised airflows were deflected from the bottom and ascended to the upper level of the room, forming expanded air recirculation regions. According to the current view, MV 2 and MV 3 had much stronger airflow movement across the room, implying that such a large turbulent region may potentially carry more droplets throughout the room. CV 1 and CV 2 could yield a more localised mixing airflow pattern due to closer vent locations. It was discovered that in CV 1, the supply air could quickly converge to the room center from the edge, whereas in CV 2, the gathered inlets generated a more intense airflow pattern, resulting in a large vortex in the center. Both these two centralised ventilation schemes resulted in a number of air recirculation zones.

The airflow pattern at the susceptible occupants' breathing level was further demonstrated in Fig. 4. It can be

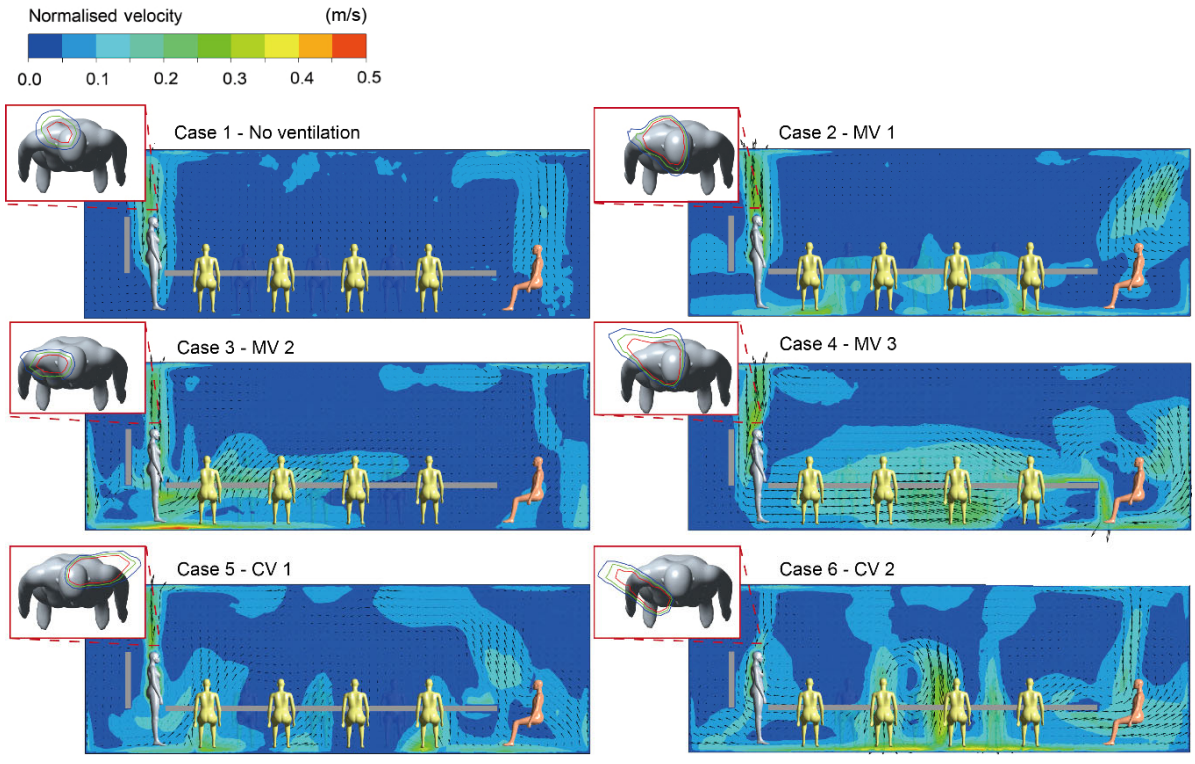

Fig. 3 Airflow pattern along *XZ* plane induced by 6 ventilation strategies.

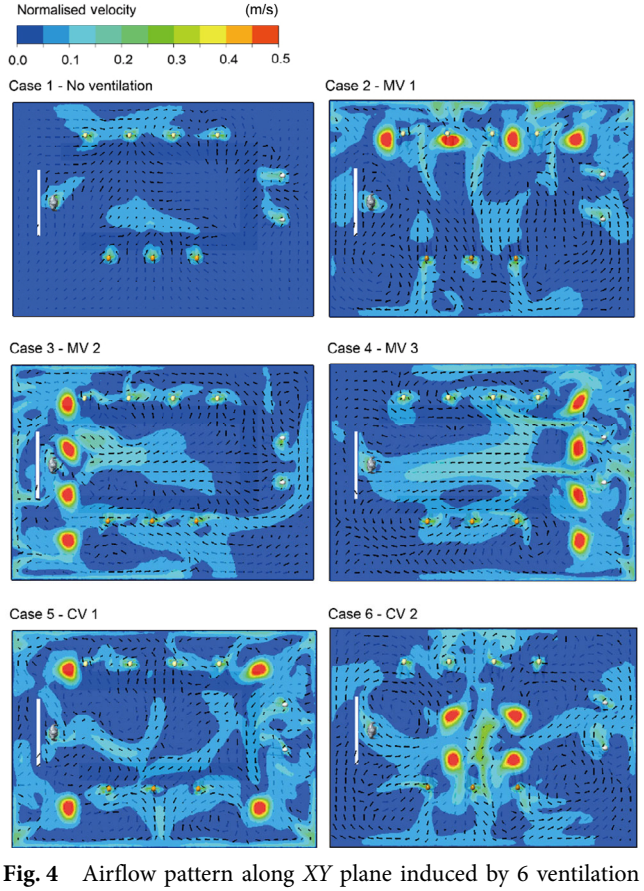

Fig. 4 Airflow pattern along *XY* plane induced by 6 ventilation strategies.

clearly noticed that the jet flow induced by the ventilation inlets could significantly break up the local airflow field of the occupants who were sitting close to the inlets. It can be speculated that droplets released close to such airflow pattern could travel more widely and intensely in the indoor space. In addition, five mixing ventilations could all induce different degrees of the vortex region in the vicinity of the occupants. Such vortex regions inferred that droplet trapped in these areas would be potentially locked and their residence time may substantially be increased.

To elucidate the droplet release process of the infectious agent and its interaction with the surrounding environment, the development of the cough droplets in the human local environment in the natural ventilation case was used, as illustrated in Fig. 5. It can be clearly noticed that during the cough droplet release period (at t = 0.1 and 0.5 s), the small droplets can be jointly dominated by the cough-jet and local airflow. These small cough-expelled droplets were swiftly ejected horizontally owing to the intensive cough jet and travel further even after the accomplishment of the coughing behavior (i.e., t = 0.5 s). Meanwhile, the large droplets were rapidly settled on the ground due to their significant weight and inertia. The effect of the cough jet would continuously be dissipated and the movement of the small droplets would be further jointly affected by the local thermally driven buoyancy flow. As a consequence, some droplets were first trapped in the local environment, further elevated to the upper level of the room with the ascending thermal plume.

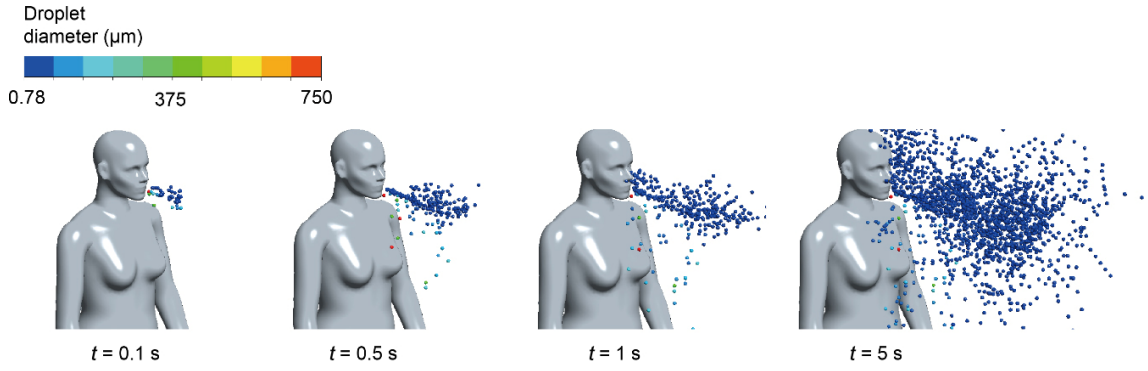

Fig. 5 Development of cough droplets in human local environment.

3.2 Cough-expelled droplet transport

Droplet suspension in the room under the effect of six ventilation strategies was further illustrated by visualising the detailed droplet trajectories, as shown in Fig. 6. It can be clearly found that without the inclusion of the ventilation, droplets would mostly be stuck at the proximity of the infectious agent after cough droplets were expelled. These droplets could travel slowly due to the stagnant airflow pattern. For traditional mixing ventilations (i.e., MV 1, MV 2, and MV 3), the performance of ventilation in containing the pathogen spread was found highly associated with the location of the droplet release. When the inlets were placed close to the infectious agents (i.e., MV 2 case), the strong jet effect of ventilated flow could vastly spread the pathogens across the room, whereas pathogens may be more effectively exhausted with a closer outlet location (i.e., MV 3 case). The droplet dispersion had a more uniform pattern with these traditional mixing ventilation schemes. In comparison, it can be found that the droplet dispersions under the effect of the CV 1 and CV 2 were more localised due to the aforementioned multiple air recirculation zones and thereby most droplets were locked in the vicinity of the infectious agent.

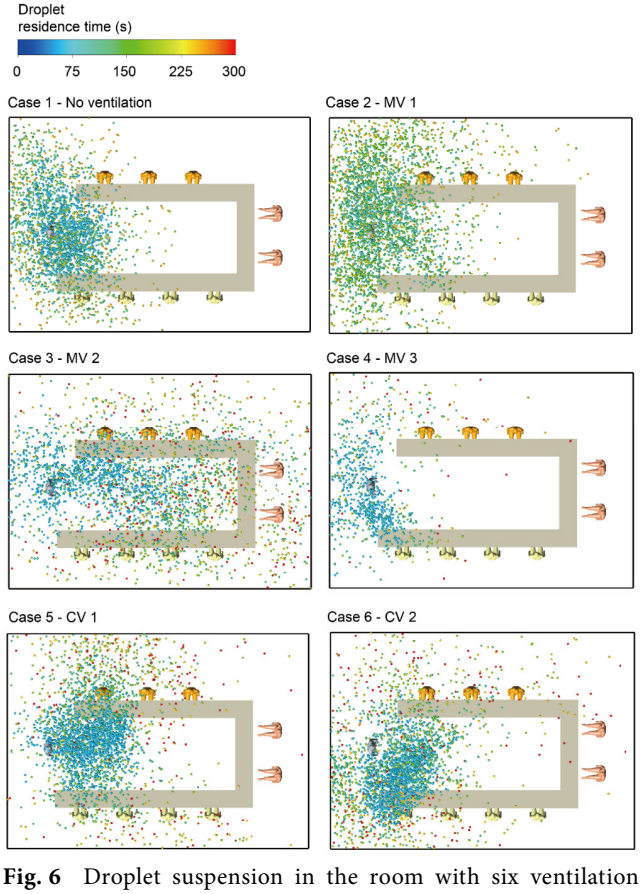

Fig. 6 Droplet suspension in the room with six ventilation strategies.

The average droplet suspension time for a given time period of 300 s was further quantitively compared, as demonstrated in Fig. 7. It can be clearly noticed that droplet suspension time was jointly dominated by droplets' physical property and environmental factors. The droplets with small initial diameter (i.e., < 40 μm) could be becoming respirable and experiencing longer suspension in the air. Beyond this size group, the medium inspirable droplets were less likely to be inhaled and their suspension time was significantly reduced with the increase of weight. However, the influence from ventilated flow and cough jet was found minimal on the larger droplets (> 200 μm) with considerable weight and inertia. Large droplets normally fell freely once released, resulting in a much shorter residence time. In terms of the ventilation performance, it can be found that traditional side mixing ventilation had a great potential to promote the droplet suspension, especially for these respirable droplets. However, when the inlet location was not conducive to pathogen spread (MV 3), pathogens could be effectively limited and the droplet's residence time were cut in half compared to the natural ventilation case. On the contrary, the mixing ventilation with a centralised vent layout could only lead to a slight reduction of droplet suspension time compared to the natural ventilation case, due to that plenty of cough-expelled droplets were blocked in the air recirculation zones.

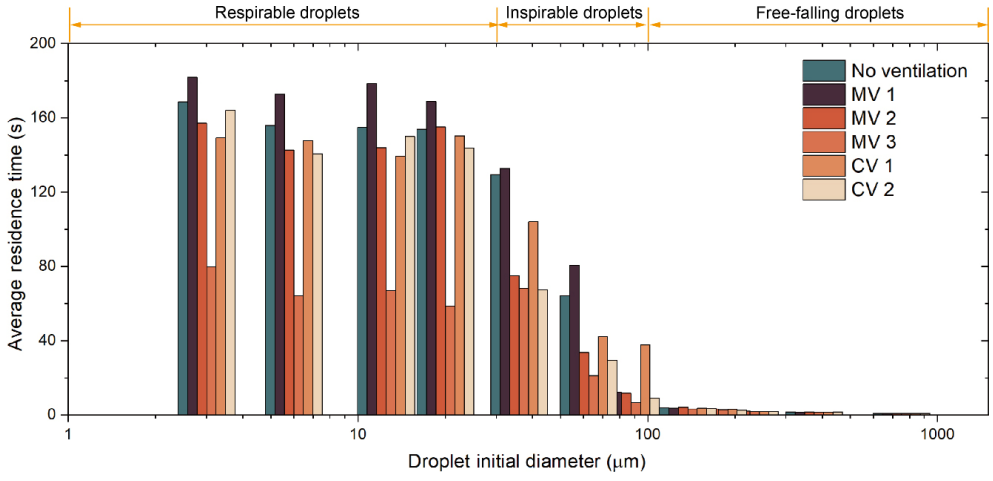

Fig. 7 Droplet's average suspension time in the conference with six ventilation strategies.

The ventilation performance in diluting the droplet concentration was further investigated, as illustrated in Fig. 8. It can be clearly noticed that most ventilation schemes could yield a more effective removal of the suspended droplets in the room compared to natural ventilation, except for MV 1. A strong downward jet flow in MV 2 could quickly remove a portion of the droplet by pushing it against the obstacles. The faster droplet removal rate in MV 3 was due to the location of the exhaust being in favor of limiting pathogen spread. More intense airflow patterns in CV 1 and CV 2 could more effectively carry suspended droplets to the close outlets. The scenario could only differ with MV 1 because the droplets may be more easily trapped in the center of the enlarged air recirculation zone produced by MV 1. Because of the low airflow momentum in the center of the airflow recirculation region, the travel time could be greatly extended.

3.3 Droplet exposure risks

The ventilation design in containing the pathogen spread indoors should always be prioritized on human's breathing zone as virus-laden droplets could not be inhaled to initiate infection until reaching the human breathing region. Figure 9 illustrates the number fraction of aerosol residue and droplet residue suspended in the occupant's breathing region for a given exposure period of 300 s.

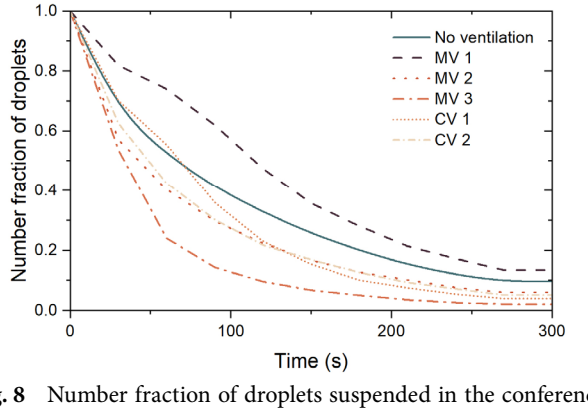

Fig. 8 Number fraction of droplets suspended in the conference with six ventilations.

For the natural ventilation case, it can be noticed that occupants sitting in the vicinity of the infectious agents could have a higher chance of inhalation of droplet residue compared to other cases. As the number of virions contained in the droplets could be exponentially increased with rising diameters, exposure risk in a room with natural ventilation could still be very significant (Riediker et al., 2022). The inclusion of ventilation may potentially promote the aerosol residue suspension in the human breathing zone. Such a phenomenon was evident in MV 2, where all susceptible occupants in the conference room were exposed to the pathogen-bearing aerosols. MV 3 was the most optimal ventilation strategy in this study as it could effectively remove the droplets from this conference room. For CV 1 and CV 2, the aforementioned airflow recirculation zone could lead to a high number of droplets suspended in the occupants' breathing region who was sitting in the proximity of the infectious agent. These two ventilation schemes would more likely restrict the droplet movement in a specific region near the infectious agent, while this would also pose certain exposure risks to the surrounding occupants due to localized vortex region. These findings indicated that the traditional mixing ventilation layout could have drastically different performance in containing virus spread as a result of changing vent location. With high uncertainty about human location or behavior in the workplace, such a ventilation scheme could not provide a controllable and stable performance in containing the virus spread. Mixing ventilation with centralised layouts, on the other hand, could offer a relatively more stable control of the airborne transmission,

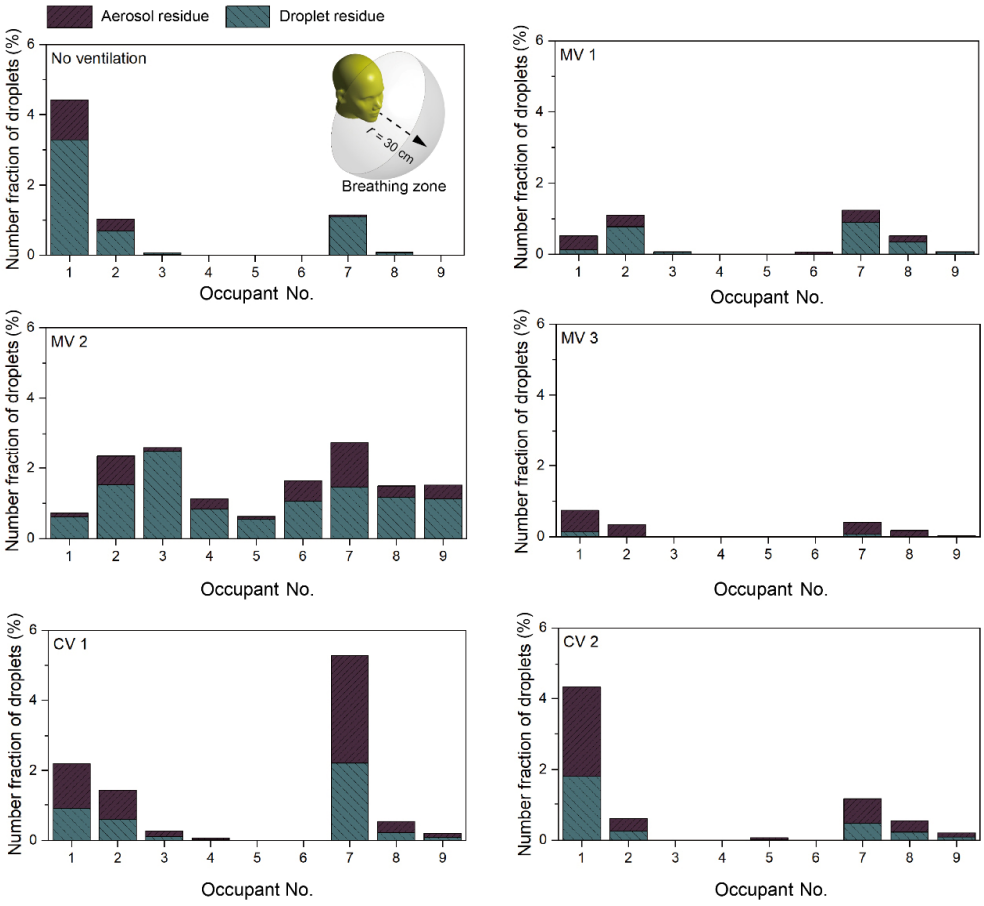

Fig. 9 Number fraction of aerosol residue (1–10 μm) and droplet residue (10–50 μm) suspended in a human micro-environment for given 300 s.

limiting the pathogen spread to the entire room. However, the occupants sitting close to the infectious agent still have higher exposure risk because of the aforementioned air recirculation zone.

Since a much higher aerosol fraction was observed in the human breathing zone, its time-dependent fraction under the effect of the ventilation strategies was further studied, as demonstrated in Fig. 10. It can be noticeable that the exposure risk of occupants increased linearly under the natural ventilation condition, whereas with the activation of the mixing ventilation schemes, the exposure risk increased exponentially. This finding suggested that a strong jet flow effect could bring substantial randomness to droplet dispersion in the human breathing zone. Such evidence revealed that the current traditional mixing ventilation layout may not provide effective and stable control of the pathogen spread over time. Mixing ventilation with centralised layouts could also fail to consistently control the occupant's exposure risk over time.

Also, it was found from Fig. 9 and Fig. 10 that the effectiveness of mixing ventilation layouts (MV 1, MV 2, and MV 3) in diluting the pathogen and lowering the occupants' exposure risk was not stable and consistent enough as the results were highly sensitive to the vent location. In comparison, temporally, although the mixing ventilation with centralised layouts was not stable and controllable enough to reduce the exposure risk of occupants, it had a great potential to provide a more consistent control of the pathogen spread from the spatial perspective. It was suggested that in the near future, ventilation design in terms of pathogen control could focus more on how to achieve more stable performance (e.g., reducing the effect of droplet release locations).

4 Conclusions

This study numerically investigated the occupant's health and safety in the typical indoor environment by considering the realistic conference scenarios. The time-dependent cough flow and droplet was released from an infectious agent with standing posture (speaker) and nine sitting occupants were employed as the susceptible individuals. The effectiveness of natural and various mixing ventilations in diluting the pathogen concentration and controlling the

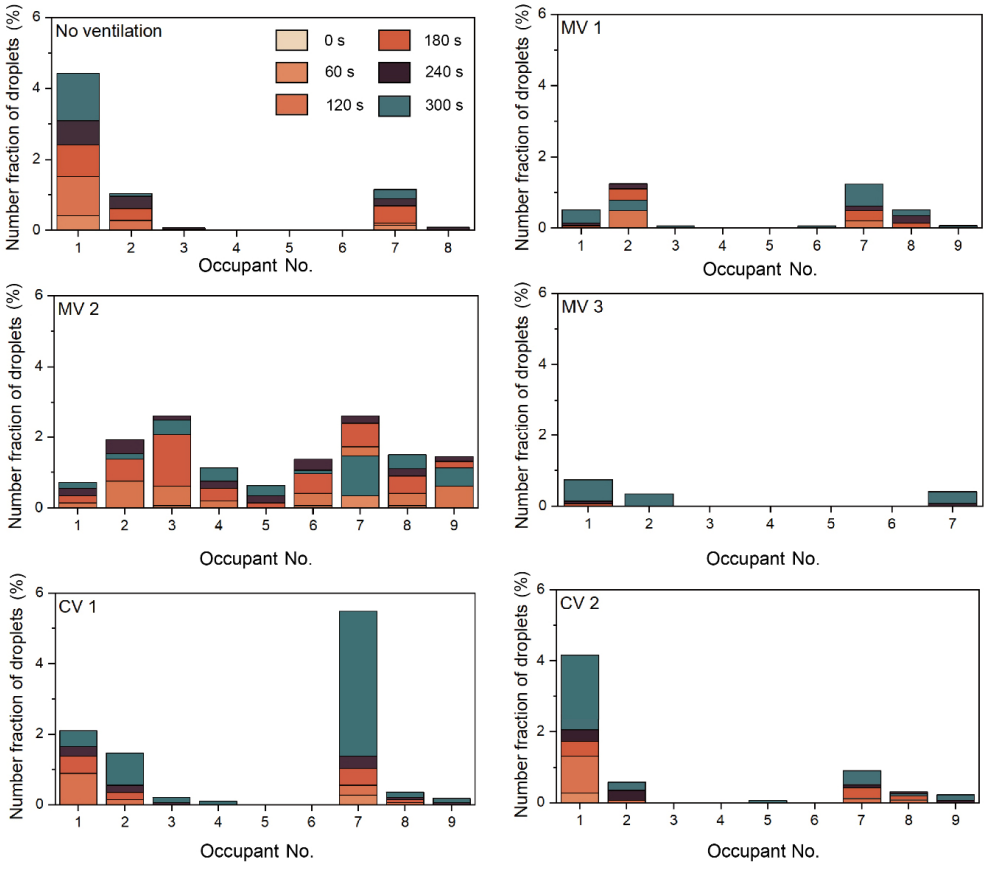

Fig. 10 Number fraction of aerosol droplets in breathing zone with time.

exposure risks was carefully assessed by analysing the detailed trajectories of the cough-expelled droplets. Outcomes from this study were concluded as follows:

1) Droplet residue with an initial diameter smaller than 40 μm was found to have great potential to reach the occupants' breathing region. The suspension of aerosol residue (< 10 μm) in the breathing zone could be even nearly doubled as a result of ventilation. In some scenarios (e.g., MV 2), all susceptible occupants were found exposing to the pathogen-bearing droplets within 300 s of exposure. Social distancing would be less effective under such ventilation layouts.

2) The traditional mixing ventilation with side-vent layouts was found to be highly sensitive in controlling the droplet dispersion. It revealed that when the inlets were located close to the infectious agent, the strong ventilated jet flow could significantly promote the droplet spread. As a possible solution, the location of the outlets should be designed as close as possible to the upward side of the presenter.

3) The centralised mixing ventilation could provide relatively more consistent performance in controlling the occupant's exposure risks from the spatial standpoint as it could discretise the entire room into several airflow field regions, limiting the pathogen spread across the entire room. However, it was worth noting that such airflow pattern could create air recirculation zone that could potentially trapping the droplets in some occupants' local environment. Future ventilation design optimisation should put more emphasis on how to minimise the droplet local lock-up phenomena and to achieve more consistent control of occupants' exposure risks.

Declaration of competing interest

The authors have no competing interests to declare that are relevant to the content of this article.

References

Allen, J. G., Ibrahim, A. M. 2021. Indoor air changes and potential implications for SARS-CoV-2 transmission. *JAMA*, 325: 2112–2113.

Anderson, E. L., Turnham, P., Griffin, J. R., Clarke, C. C. 2020. Consideration of the aerosol transmission for COVID-19 and public health. *Risk Analysis*, 40: 902–907.

ASHRAE. 2011. *ASHRAE Handbook—HVAC Applications*.

Carvalhais, C., Querido, M., Pereira, C. C., Santos, J. 2021. Biological risk assessment: A challenge for occupational safety and health

practitioners during the COVID-19 (SARS-CoV-2) pandemic. *Work*, 69: 3–13

Chao, C. Y. H., Wan, M. P., Morawska, L., Johnson, G. R., Ristovski, Z. D., Hargreaves, M., Mengersen, K., Corbett, S., Li, Y., Xie, X., et al. 2009. Characterization of expiration air jets and droplet size distributions immediately at the mouth opening. *Journal of Aerosol Science*, 40: 122–133.

Chen, Q. 1995. Comparison of different k–ε models for indoor air flow computations. *Numerical Heat Transfer, Part B: Fundamentals*, 28: 353–369.

Fan, Y., Li, X., Yan, Y., Tu, J. 2017. Overall performance evaluation of underfloor air distribution system with different heights of return vents. *Energy and Buildings*, 147: 176–187.

Greenhalgh, T., Jimenez, J. L., Prather, K. A., Tufekci, Z., Fisman, D., Schooley, R. 2021. Ten scientific reasons in support of airborne transmission of SARS-CoV-2. *The Lancet*, 397: 1603–1605.

Gupta, J. K., Lin, C. H., Chen, Q. 2009. Flow dynamics and characterization of a cough. *Indoor Air*, 19: 517–525.

Johns Hopkins University. 2020. COVID-19 dashboard by the Center for Systems Science and Engineering (CSSE) at Johns Hopkins University (JHU). Available at https://coronavirus.jhu.edu/map.html.

Katella, K. 2021. Comparaing the COVID-19 vaccines: How are they different? Available at https://www.yalemedicine.org/news/covid-19-vaccine-comparison.

Licina, D., Pantelic, J., Melikov, A., Sekhar, C., Tham, K. W. 2014. Experimental investigation of the human convective boundary layer in a quiescent indoor environment. *Building and Environment*, 75: 79–91.

Lipinski, T., Ahmad, D., Serey, N., Jouhara, H. 2020. Review of ventilation strategies to reduce the risk of disease transmission in high occupancy buildings. *International Journal of Thermofluids*, 7–8: 100045.

Lu, J., Gu, J., Li, K., Xu, C., Su, W., Lai, Z., Zhou, D., Yu, C., Xu, B., Yang, Z. 2020. COVID-19 outbreak associated with air conditioning in restaurant, Guangzhou, China, 2020. *Emerging Infectious Diseases*, 26: 1628–1631.

Miller, S. L., Nazaroff, W. W., Jimenez, J. L., Boerstra, A., Buonanno, G., Dancer, S. J., Kurnitski, J., Marr, L. C., Morawska, L., Noakes, C. 2021. Transmission of SARS-CoV-2 by inhalation of respiratory aerosol in the Skagit Valley Chorale superspreading event. *Indoor Air*, 31: 314–323.

Mittal, R., Ni, R., Seo, J. H. 2020. The flow physics of COVID-19. *Journal of Fluid Mechanics*, 894: F2.

Motamedi, H., Shirzadi, M., Tominaga, Y., Mirzaei, P. A. 2022. CFD modeling of airborne pathogen transmission of COVID-19 in confined spaces under different ventilation strategies. *Sustainable Cities and Society*, 76: 103397.

Nicas, M., Nazaroff, W. W., Hubbard, A. 2005. Toward understanding the risk of secondary airborne infection: Emission of respirable pathogens. *Journal of Occupational and Environmental Hygiene*, 2: 143–154.

Peng, S., Chen, Q., Liu, E. 2020. The role of computational fluid dynamics tools on investigation of pathogen transmission: Prevention and control. *Science of The Total Environment*, 746: 142090.

Riediker, M., Briceno-Ayala, L., Ichihara, G., Albani, D., Poffet, D., Tsai, D. H., Iff, S., Monn, C. 2022. Higher viral load and infectivity increase risk of aerosol transmission for Delta and Omicron variants of SARS-CoV-2. *Swiss Medical Weekly*, 152: w30133.

Sheriff, R. E. 2020. Building ventilation – The proper air changes per hour (ACH). Available at https://www.atlenv.com/building-ventilation-the-proper-air-changes-per-hour-ach.

Sohrabi, C., Alsafi, Z., O'Neill, N., Khan, M., Kerwan, A., Al-Jabir, A., Iosifidis, C., Agha, R. 2020. World Health Organization declares global emergency: A review of the 2019 novel coronavirus (COVID-19). *International Journal of Surgery*, 76: 71–76.

Wang, C. C., Prather, K. A., Sznitman, J., Jimenez, J. L., Lakdawala, S. S., Tufekci, Z., Marr, L. C. 2021. Airborne transmission of respiratory viruses. *Science*, 373: eabd9149.

Wei, J., Li, Y. 2015. Enhanced spread of expiratory droplets by turbulence in a cough jet. *Building and Environment*, 93: 86–96.

World Health Organization. 2020a. Coronavirus disease (COVID-19) outbreak: Rights, roles and responsibilities of health workers, including key considerations for occupational safety and health: Interim guidance. Available at https://apps.who.int/iris/handle/10665/331510.

World Health Organization. 2020b. Transmission of SARS-CoV-2: Implications for infection prevention precautions. Available at https://www.who.int/news-room/commentaries/detail/transmission-of-sars-cov-2-implications-for-infection-prevention-precautions.

World Health Organization. 2021. Advice for the public: Coronavirus disease (COVID-19). Available at https://www.who.int/emergencies/diseases/novel-coronavirus-2019/advice-for-public.

Yan, Y., Li, X., Yang, L., Tu, J. 2016. Evaluation of manikin simplification methods for CFD simulations in occupied indoor environments. *Energy and Buildings*, 127: 611–626.